

## NUMERICAL MODELLING OF ISOTHERMAL BURNER JETS

James HART<sup>1,2</sup>, Jamal NASER<sup>1,2</sup>, Peter WITT<sup>1,3</sup> and Louis MITTONI<sup>1,3</sup>

<sup>1</sup> CRC – Clean Power from Lignite, Mulgrave, Victoria 3170, AUSTRALIA

<sup>2</sup> Swinburne University of Technology, Hawthorn, Victoria 3122, AUSTRALIA

<sup>3</sup> CSIRO Minerals, Clayton, Victoria 3169, AUSTRALIA

### ABSTRACT

Isothermal slot burners, based on those found in conventional coal fed tangentially fired furnaces, have been numerically modelled using the Computational Fluid Dynamics (CFD) code CFX 4.2. Three different burner geometries have been studied in detail, and the predictions are compared to the existing data obtained experimentally for the same geometries.

An orthogonal grid arrangement was constructed for the first geometry, minimising complications due to numerical diffusion that can impact heavily on predictions. Good agreement between CFD prediction and experimental data was achieved with this geometry, even using a simple  $k-\epsilon$  turbulence model and first order differencing scheme. The grid for the second geometry was more complex because the jet discharged at an angle to the computational domain, and grid orthogonality was not inherent in the problem set up as it was in the first geometry. Good agreement was still obtained between the predictions and the experimental data. However, higher order differencing schemes such as bounded quadratic schemes, and more complex turbulence models are required to achieve more accurate predictions. Typical differences between the predictions and experiment were of the order of 10 to 15%

A third burner geometry was modelled, which contained a recess into which the jets discharged. This introduced complex flow behaviour, which was correctly predicted in a two dimensional model.

### NOMENCLATURE

$X$  Distance downstream of jet exit plane  
 $d$  Hydraulic diameter of duct  
 $U$  velocity  
 $U_{ce}$  Centre line exit velocity

### INTRODUCTION

Whilst new technologies for coal combustion are being investigated for future use, existing technologies such as pulverised fuel (p.f.) fired furnaces are still heavily used, and require constant refinement to improve efficiency, and ensure compliance with prescriptive environmental emission standards.

The near burner region in a conventional boiler is very important, as it is in this region that parameters such as entrainment, and mixing rates of the fuel laden jet with the

surrounding hot combustion gases, determine the combustion characteristics of the boiler. The effects of burner geometry on both flame stability and mixing are important, but not completely understood. It is highly desirable for any CFD model of a conventional p.f. fired furnace to be capable of accurately predicting the aerodynamics of the burner region, in order to accurately model combustion in the furnace.

Detailed experimental studies have been conducted by Perry and Hausler (1982), and Perry *et al* (1986) to investigate the effects of burner geometry on aerodynamics. Further research on the effect of particles in the jet stream was performed by Yan and Perry (1994). The present research aims to model isothermal burner jets, for ultimate use in the CFD model of a tangentially fired p.f. furnace.

### MODEL DESCRIPTION

The isothermal slot burners being modelled are based on the burners used in a series of experiments by Perry (1982). Extensive velocity profile measurements were acquired for four different burner geometries, providing a firm basis for validation of CFD simulations. It is important to ensure that the CFD model accurately represents the physical set up of the experimental apparatus in order to be able to confidently compare the predictions with experimental data.

The experimental facility, which was the same as the solution domain used in the present study, consists of a tri-jet configuration, with one primary jet, flanked on the top and bottom by two smaller secondary jets. The nozzle duct system maintains the cross-section of the nozzle exit for 52 hydraulic diameters upstream, to ensure a fully developed profile at the exit plane (Perry, 1982). The three jets then discharge from the centre of a large wall into an open atmosphere. The different geometry types modelled as illustrated in Figure 1 were:

- a) Geometry A: A three-jet system where the burner face is located at the boiler wall and the jet exit flow direction is normal to this wall
- b) Geometry B: As for Geometry A but with the jet flow direction set at 60° to the boiler wall.
- c) Geometry D: As for Geometry B but with the jet exit recessed into a cavity in the boiler wall, and the sides of the cavity diverging at an angle of 10°.

The experimental jets discharged into an open atmosphere, which means that the boundary conditions extend to infinity, at least theoretically. This is difficult to implement numerically, and so the “infinite” experimental domain was truncated to give a computational domain of reasonable size. A constant pressure boundary condition is used which applies Neumann conditions to the velocity. The boundaries must be situated far enough from the jet so as to preclude them from significantly influencing the computation.

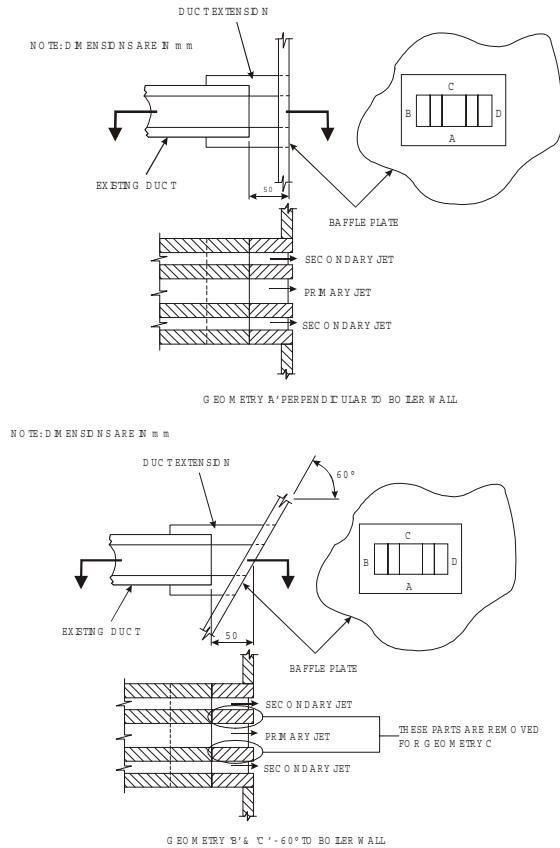


**Figure 1:** Experimental Duct Layout from Perry (1982)

### Numerical Methods

CFX-4.2 was used in this study. It is a commercial finite volume CFD code. The SIMPLEC algorithm (Van Doormal and Raithby, 1984) was used for velocity/pressure coupling and the Rhie-Chow interpolation method to avoid checkerboard oscillations on the co-located grid. Reynolds time averaging is implemented to smooth out turbulent fluctuations. CFX-4.2 utilises a non-orthogonal body fitted coordinate system to enabling complex geometries to be gridded.

Of the numerous differencing schemes available in CFX-4.2, the ones used in this paper are; Hybrid, Higher Upwind and two bounded higher order differencing schemes; CCCT and Van Leer. Hybrid is a first order accurate scheme, and is very stable. However, it is prone to allowing false diffusion to influence the solution. To combat false diffusion, higher order schemes such as Higher Upwind, CCCT and Van Leer were used. Higher order schemes reduce false diffusion, but are less stable and can generate non-physical solutions to some equations. To remedy this, CCCT and Van Leer include limiting terms to

prevent the possibility of non-physical overshoots in their solutions.

### Turbulence Models

The two equation  $k-\epsilon$  turbulence model provides a computationally stable and readily solvable model which can easily generate a solution, but it suffers from the assumption of isotropic turbulence (turbulent fluctuations are the same in all directions). In a number of cases this assumption is invalid, and often leads to inaccurate modelling in regions of anisotropy. However, because it can generate a reasonably accurate solution relatively quickly, it can be used to provide an initial guess for other turbulence models like the Reynolds Stress Model (RSM). The RNG  $k-\epsilon$  model is an alternative to the standard  $k-\epsilon$  model for high Reynolds number flows. A modification is made to the equation for  $\epsilon$  and contains a different set of model constants to standard  $k-\epsilon$ . This model is marginally more computationally expensive than the standard  $k-\epsilon$  model.

The Reynolds Stress Model solves transport equations for each of the six Reynolds stress tensors, instead of defining them in terms of the eddy viscosity. Solving six extra transport equations significantly increases the computational burden of the problem, but often leads to a more accurate solution because the anisotropic nature of the turbulent fluctuations it accounted for. Although the isothermal slot burners do not contain any strongly swirling flows, for which the Reynolds Stress model is definitely superior over the  $k-\epsilon$  model, there are several regions in the jet where anisotropy of turbulence is expected, so use of the Reynolds stress model was justified.

## RESULTS AND DISCUSSION

### Geometry A

Geometry A discharges at  $90^\circ$  to the wall, allowing for an orthogonal grid to be easily set up where the direction of bulk flow of the jet is aligned with the grid. False diffusion occurs when the flow direction is incident at an angle to the face of the control volume, because lower order differencing schemes treat the flow as locally one-dimensional. If the flow is not one-dimensional across the cell, the differencing schemes incorrectly represent the true convective nature of the flow. An aligned grid will not completely remove the effects of inaccuracies in the differencing scheme, but it will remove false diffusion.

Two grid arrangements were used in order to demonstrate grid independency. A typical arrangement is shown in a three-dimensional diagram of the model geometry in Figure 2.

The grid was set up using a multi-block strategy in order to concentrate the cells in the regions of the flow where gradients are high, and fine resolution is required. Once the grid was generated, the pre-processor CFX Meshimport was used to reduce the number of blocks, hence decreasing the amount of inter-block communication required by the solver and increasing the block size which allows better vectorisation of the code, and a more rapid solution.

The coarser of the two grids was 4x4 cells in the cross section of the main duct, and 2x4 cells across the secondary ducts. The rest of the grid was generated by progressively enlarging the cells away from the duct exit plane, whilst ensuring that the rate of change of cell size did not become too large so as to reduce the chance of numerical instabilities. This generated a grid of approximately 400,000 cells, in a domain of 5m x 2m x 2m, while ensuring grid integrity is preserved.

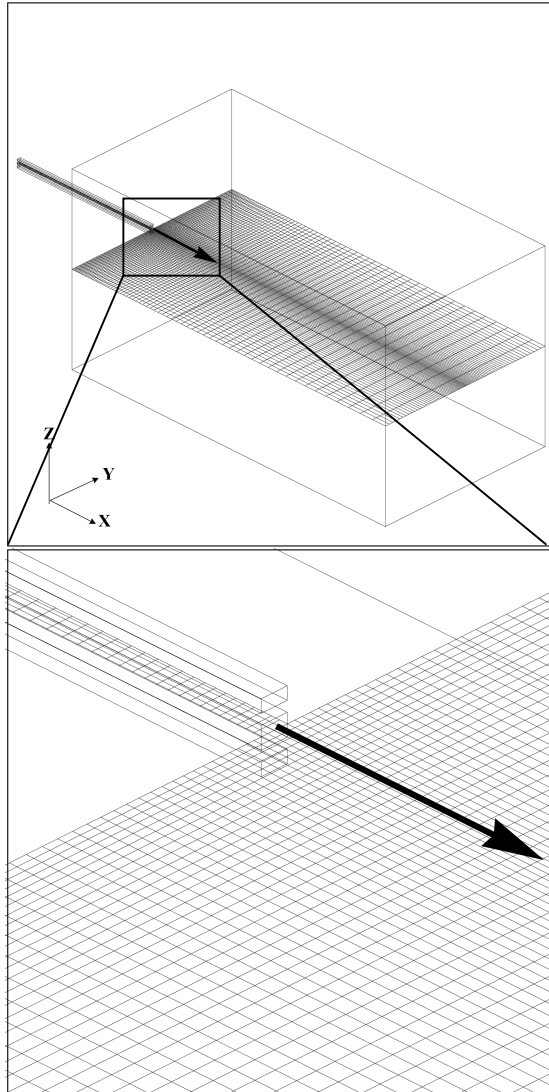


**Figure 2:** Diagram of Model Geometry

A second, finer grid was generated, where the number of cells on the cross section of the duct was doubled to 8x8 for the main, and 4x8 for the secondary jets. This corresponded to a smoothly changing grid of approximately 1,000,000 cells for the whole domain.

#### **Grid Independence**

Figure 3 shows the predicted velocity profiles taken from the XY plane slicing through the main duct, at two downstream positions,  $X/d = 0$  and  $X/d = 9$ , where  $d$  is the hydraulic diameter of the main duct, and  $X$  is the distance downstream of the duct exit. The velocities are normalised to the maximum velocity on the centerline of the jet on the duct exit plane. The position  $X/d = 9$  has been chosen

because this is the data set furthest downstream available from the experiment, and any variation between the two predictions should be greatest at this point because the predicted jet is expected to diffuse downstream of the expansion. Hybrid differencing and k-ε turbulence models were used.

The maximum variation between the velocity profiles at  $X/d = 9$  for the coarse and the fine grid is 15% at  $|y/d| > 1.4$ . However, considering that the grid size has more than doubled, the variation is not significant. Here the solution can be assumed to be very nearly grid independent.

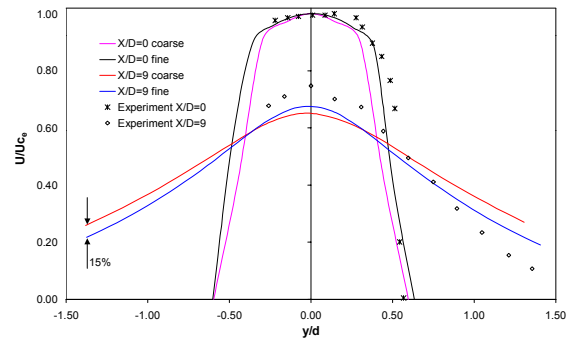


**Figure 3:** Predictions for Two Grid Sizes

Due to limitations of the computer no further increase in cell number could be afforded. To ensure the most accurate solution, the finer grid arrangement with 1,000,000 cells was used in the subsequent study

#### **Comparison with Experiment**

Figure 3 shows the comparison of the model with the velocity profiles from the experiment of Perry (1982), at 0 and 9 diameters downstream of the nozzle exit plane. The model uses hybrid differencing and the k-ε turbulence model, on the fine grid. Small differences between the model and the experiment are evident. The profile at the exit plane where  $X/d = 0$ , is very close to the experiment, which provides confidence that the number of cells used for the duct cross section is sufficient.

The major difference appears 9 diameters downstream of the duct exit, where the model predicted a lower, fatter profile than the experimental results. The peak centre line velocity was under predicted, and at  $y/d > 0.8$  the velocities were over predicted by about 30%. Physically, this means the jet was not penetrating as far and was spreading more than the experimental jet. The cause of these discrepancies can be explained by false diffusion, whereby the diffusion term from the momentum transport equation, is being made large and the model jet was diffusing to the sides, instead of conserving momentum and penetrating further. Another possible cause of these discrepancies is the turbulence model used. The k-ε turbulence model is known to be overly diffusive and may have contributed to the spread of the jet.

Figure 4 displays the improved profile at  $X/d = 9$  obtained using a second order differencing scheme for linearizing the transport equations as opposed to the first order hybrid scheme used previously. Van Leer is a bounded higher order quadratic differencing scheme. The addition of this scheme marginally improved the model accuracy over the

hybrid differencing scheme, because hybrid differencing should not cause large false diffusion errors if the flow is aligned with the grid. However, the flow here was not perfectly aligned with the grid, due to some entrainment from the surroundings.

The standard k-ε model in some cases incorrectly predicts the turbulent properties of the flow, because of assumptions made in the Eddy Viscosity Hypothesis. The Reynolds stress model, which solves transport equations for all six Reynolds stress components of turbulence, instead of simply modelling them all through the eddy viscosity hypothesis, is often considered to be a more accurate turbulence model. Figure 4 shows the modelling results with the addition of the Reynolds stress model in lieu of the k-ε model. There is a marked improvement in the profile from the centerline to  $y/d \pm 0.9$ , differing from the experiment by less than 10%. However, at  $y/d > 0.9$  it becomes only slightly better than the k-ε model and is still over predicting by around 30%. Figure 4 also shows the Reynolds stress model used in conjunction with another bounded third order differencing scheme, CCCT. The use of this differencing scheme had almost no effect on solution. This is expected, as the hybrid scheme should not introduce significant false diffusion errors on an orthogonal grid.

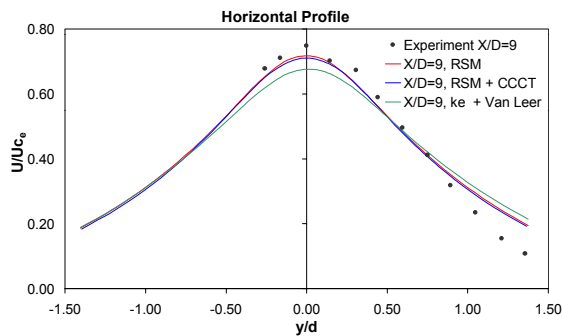


**Figure 4:** Fine Grid Predictions with Different Combinations of Differencing Scheme and Turbulence Model

The velocity profile at  $X/d = 9$  does not show perfect agreement with the experimental results at  $|y/d| > 0.9$ . This discrepancy can be accounted for by the grid, by diffusion due to the turbulence models and by experimental error. At  $y/d$  ratio of  $\geq 0.5$  means that the point lies outside the width of the duct, and the grid resolution past this point gets progressively coarser, which could contribute to inaccurate predictions by the model. By ensuring the cell sizes in this region stayed closer to those of the duct cross section for a longer distance around the duct, this problem may be avoided.

These results illustrate that by simply using the Reynolds stress model on a grid with 8 cells across the inlet, and 1,000,000 cells in total, an accurate numerical model can be constructed which matches well with the experimental results. However, the Reynolds stress model is computationally more expensive than the k-ε model, because it solves five additional transport equations.

Figure 5. shows the velocity profile taken through the YZ plane, on the centerline of the ducts. The left peak is one

of the secondary ducts, and the larger peak on the right is the main duct. Again data is taken from  $X/d = 0$  and 9. At 9 diameters downstream the model prediction is very good compared with the experiment for the region in the middle of the jet, corresponding to the main duct. In the region of the secondary jet, however, the model under predicted the jet velocities, and again it is shown to be too diffusive at the edges.

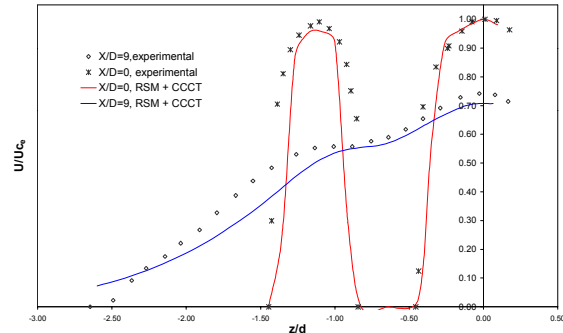


**Figure 5:** Vertical Profile with RSM Model

The velocity gradients in the centre of the jet are relatively flat compared with the steep gradients on the outer edges of the jet. These steep velocity gradients cause a high shear, which the turbulence models do not predict very well. The models tend to cause the shear gradient to be flatter and more spread than it should be, giving a more diffusive jet.

### Geometry B

The burner jets in Geometry B discharge at an angle of  $60^\circ$  to the wall, which introduced significant false diffusion to the problem. Based on the results from Geometry A, a grid of 1,000,000 cells was used, however the dimensions of the model were slightly different. A symmetry plane was included which cuts through the main jet in the XY plane. This doubled the number of cells available for use by halving the domain and allowed for a slightly larger domain to be used. The jets were slightly offset from the centre of the domain in the XY plane to allow the jets to be fully contained in the domain, without being partially cut off by boundaries.

Again several numerical schemes have been utilised to predict the jets, utilising two differencing schemes and three turbulence models, standard k-ε, RNG k-ε and the RSM model. Results were obtained for all but the RSM model, which did not converge satisfactorily, and under some conditions even became divergent. Figure 6 shows the velocity profiles of Geometry B at an  $X/d$  position of 9 in the horizontal plane. The centre line of the jet was found by inspection from a contour plot of velocity, and was found to turn up to  $10^\circ$  away from the geometric axis. This was confirmed from the experimental results (Yan and Perry, 1994) and was due to uneven entrainment of the surrounding fluid pushing the jet towards the wall.

Model predictions for Hybrid differencing and the higher order schemes with the k-ε turbulence model showed poor agreement with the experimental profile at 9 diameters downstream of the exit plane. The higher order differencing schemes were a significant improvement over

the hybrid scheme, but they still lacked the level of agreement achieved with the same schemes in Geometry A. Several schemes were used with the k- $\epsilon$  model, and each gave the same prediction. The improvement due to the higher order schemes indicates that numerical diffusion played an important role in this jet, but the type of scheme used made little difference to the prediction.

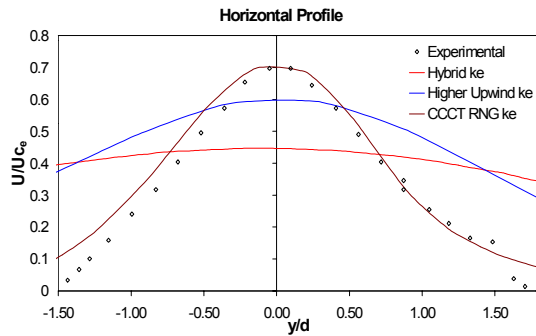


**Figure 6:** Predictions for Geometry B

The RNG k- $\epsilon$  turbulence model coupled with a third order differencing scheme shows excellent agreement with the experimental profile, differences between prediction and experiment are less than 5%. As in Geometry A the edges of the jet did not show the same sharp drop to zero velocity as the real jet, and the predicted jet appeared to be slightly squashed from the positive Y direction. This is the same direction from which the jet gets pushed towards the wall due to uneven entrainment, and is the likely cause of the disfigurement.

Results are unavailable for the RSM turbulence model because the problem either did not converge to a satisfactory level or it diverged. The reason for which is not completely understood, however it is suspected that the cross-derivate diffusion terms in the Reynolds stress and  $\epsilon$  equations are the cause (CFX Manual).

### Geometry D

Based on flow visualisation results from Perry (1982) the flow development in Geometry D is complex. For equal velocity ratios between the primary and secondary ducts, the secondary jets are separated from the short face (low Y direction) and attached to the long face (high Y) and upper and lower faces (high and low Z) of the cavity. The primary jet is separated from the long face, although this can be hard to detect. Ambient fluid entrainment occurs in the separation regions (Perry, 1982).

The angled expansion of Geometry D and the separation that is expected to occur there are likely to cause difficulties with the standard k- $\epsilon$  model because the law of the wall does not always hold under these conditions due to the adverse pressure gradient experienced by the flow. This geometry also differs from those previous by the inclusion of a small step at the entrance to the cavity, which will help trigger separation of the flow from the cavity wall. To correctly model this jet requires at least one cell width in the region of the step, which substantially increases the number of cells required for the whole cavity. To determine the minimum number of cells required to correctly model the flow in the cavity, a two

dimensional model of the primary jet was constructed. At the time of publication only two grids had been tested; one with 4 cells width in the step region which gives a grid of 60 cells across the width of the cavity, and a grid of two cells width in the step which gives 30 cells across the cavity. The finer of the two grids is displayed in Figure 7.

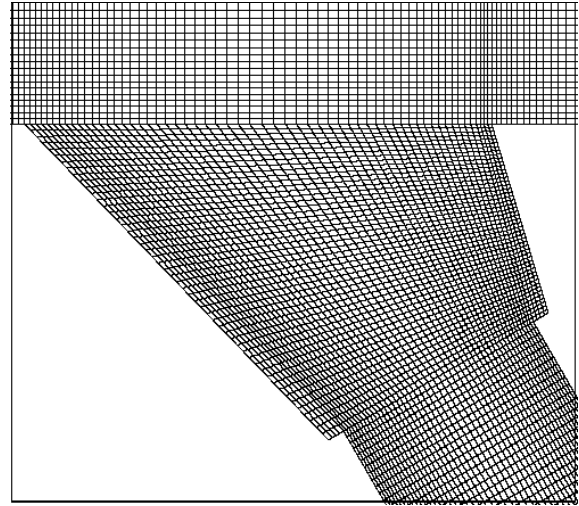


**Figure 7:** Grid Arrangement in Cavity for Geometry D

Using 60 cells across the cavity goes some way to integrating to the wall, although this is not quite possible to do properly without increasing the number of cells required to a prohibitively high number, in an already large problem. Figure 8. shows the speed contours of the fine grid using the low Reynold's number version of the  $k\omega$  model. Separation is seen on both sides of the cavity.

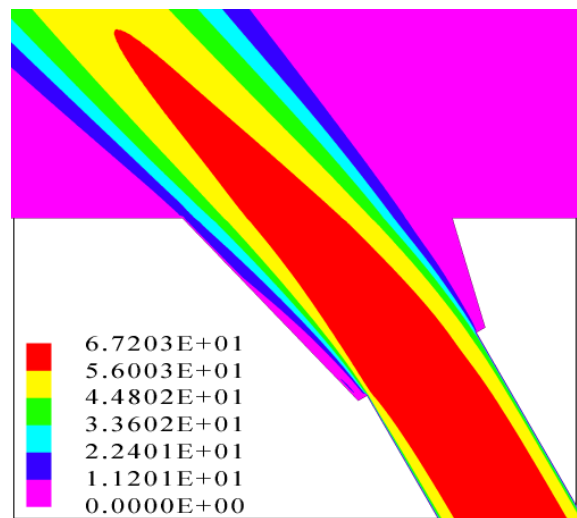


**Figure 8:** Speed Contours for 2D Jet on Fine Grid

Figure 9. shows the velocity vectors for the same flow, illustrating the reverse flow into the cavity along the long face. Figure 10. shows the speed contours for the jet on a course grid, and figure 11. shows the velocity vectors for that grid. The extent of recirculation predicted on the coarser grid is less than that for the finer grid, however it is still present. Work on this model is ongoing and will include the use of a three dimensional model when the grid requirements for correct prediction are finalised.

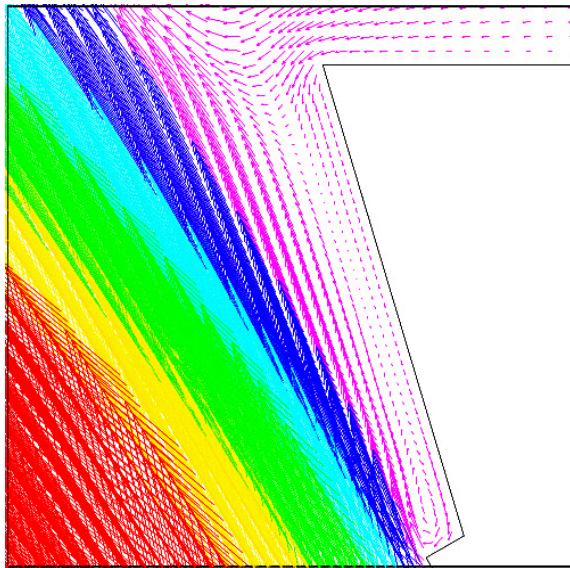


**Figure 9:** Velocity Vectors for 2D Jet on Fine Grid.

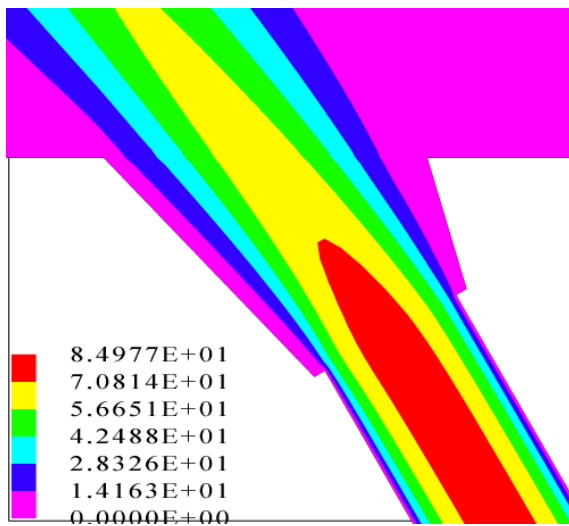


**Figure 10:** Speed Contours for 2D Jet on Coarse Grid

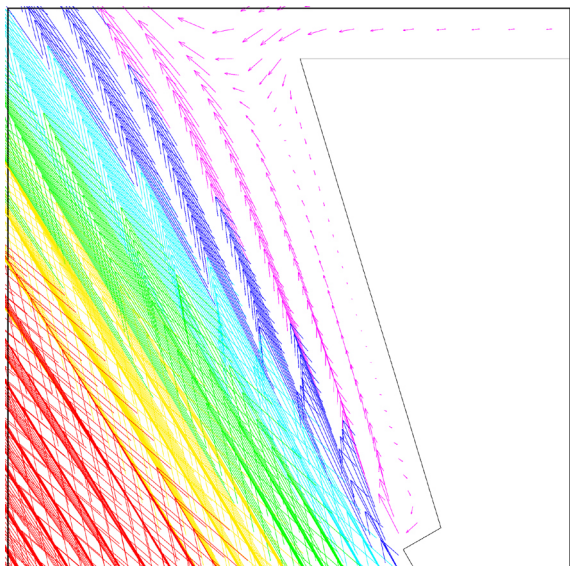


**Figure 11:** Velocity Vectors for 2D Jet on Coarse Grid

## CONCLUSION

Several numerical differencing schemes and turbulence models of differing complexity have been used to model the flow of tri-jet burners. Highly accurate predictions have been achieved for a burner of type Geometry A due to the aligned nature of the grid, using the Reynolds stress turbulence model, without higher order differencing schemes. There were some effects from the high shear layer at the boundary between the jet and the surrounding fluid, and the CFD prediction did not model this aspect of the jet very well.

Accurate predictions for Geometry B have also been achieved, with the grid at an angle of 30° to the flow direction. Although the RSM turbulence model was unable to produce a solution, possibly due to the cross-derivative diffusion terms, the RNG k-ε model gave excellent predictions with the addition of higher order differencing schemes.

Some preliminary two dimensional modelling of Geometry D gave an indication of the number of cells required to accurately predict separation in the cavity of the burner. Qualitative results matched the experimentally observed flow behaviour for the primary jet and is encouraging.

Further work will be done on the Geometry B. This will include the introduction of particles to the flow and making the jet experience cross flow, to simulate flow in a furnace situation, and the use of different primary to secondary jet velocity ratios.

## ACKNOWLEDGEMENTS

The authors gratefully acknowledge the financial and other support received for this research from the Cooperative Research Centre (CRC) for Clean Power from Lignite, which is established and supported under the Australian Government's Cooperative Research Centres program.

## REFERENCES

- CFX-4.2, (1997). User Guide – Solver, AEA Technology, Harwell Laboratory, Oxfordshire, UK.
- VAN DOORMAL, J.P., and RAITHBY, G.D., (1984), "Enhancements of the SIMPLE Method for Predicting Incompressible Fluid Flows", *Numerical Heat Transfer*, 7, 147-163
- PERRY, J. H. and HAUSLER, T., (1982), "Aerodynamics of Burner Jets Designed for Brown Coal Fired Boilers", *Report for NERDDC Grant No. GO/83/57*.
- PERRY, J. H. and HAUSLER, T., (1986), "Aerodynamics of Burner Jets Designed for Brown Coal Fired Boilers - Part V", *Final Report for NERDDC Grant No. ND/86/029*.
- YAN, H. and PERRY, J. H., (1994), "Two-Phase Flow Development in Slot Burners - Part 2 Detailed Flow Measurement and Numerical Model Validation", *ESAA Report No. ES/94/01*.